

Water transfer simulation of an electrolytic dehumidifier

Shuichi Sakuma · Shiro Yamauchi ·
Osamu Takai

Received: 9 February 2007 / Accepted: 11 November 2008 / Published online: 27 November 2008
© Springer Science+Business Media B.V. 2008

Abstract A model for a dehumidifying device using a solid polymer electrolyte membrane (Nafion 117, Dupont) is proposed. The dehumidifier in the model is represented by a physical model composed of a two-layer membrane and electrodes on the membrane surfaces. Measurement of the membrane weight shows that the ratio of the water content of the membrane to humidity in the surrounding air is a function of temperature under equilibrium conditions. The results for the water ratio are used for determining the parameters required for the modeling. The electrical resistance of the dehumidifier was measured and is given as a function of temperature and the membrane water content. Simulation of the characteristics of the dehumidifying device is presented and the results are found to agree with the measured characteristics of the device. We also report an attempt to determine the parameters describing the dehumidifying processes.

Keywords Dehumidifier · Physical model · Solid polymer electrolytic membrane · Water transfer

List of symbols

Variables

D	Diffusion coefficient of water in the dehumidifying element
e	Electron charge = 1.602×10^{-19} (C)
I	Current of the dehumidifying element (A)
I_{st}	Current at steady state condition (A)
J	Current density of the dehumidifying element
k_g	Coefficients relevant to the diffusion velocity of water from the air to the membrane
k_s	Coefficient relevant to the diffusion velocity of water from the membrane to the air. This is defined by $k_s = k_{s0} \exp(-W_s/RT)$
L	Thickness of the dehumidifying element (= 0.017 cm)
M_o	Molecular weight of water
$m_{g,p}$	Water mass in the space facing the anode (g)
N_A	Avogadro number = 6.02×10^{23} (mol ⁻¹)
R	Gas constant = 8.31 (Pa m ³ k ⁻¹ mol ⁻¹)
RH_{t_x}	Relative humidity at time t_x
R_m	Electrical resistance of the membrane of the device (Ω)
$p_{g,p}, p_{g,n}$	Water vapor pressure in the air facing the anode and the cathode, respectively
R_s	Electrical resistance of the dehumidifying element (Ω)
S	Area of the dehumidifying element of the device
t	Time (s)
T_g	Temperature of the gas space surrounding the dehumidifying element (K)
U_s	Applied voltage to the dehumidifying element (V)
$V_{g,p}, V_{g,n}$	Volumes of the spaces facing the anode and the cathode, respectively

S. Sakuma (✉)
Ryosai Technica Company Ltd., 8-1-1, Tsukaguchi-Honmachi,
Amagasaki City, Hyogo 661-0001, Japan
e-mail: sakuma.shuichi@ryosai.co.jp

S. Yamauchi
Mitsubishi Electric Corporation, 8-1-1, Tsukaguchi-Honmachi,
Amagasaki City, Japan

O. Takai
Nagoya University, Furocho, Chikusa-ku, Nagoya 464-8603,
Japan

W_s	Difference in potential energy between water in the air and in the element (J mol^{-1})
$\langle X \rangle_{[t_1, t_2]}$	Average value of variable X during the period from t_1 to t_2
α	The average number of water molecules carried by a proton moving to the cathode (electro-osmotic drag coefficient)
δ	Water content in the dehumidifying element represented by $\text{molH}_2\text{O}/\text{molSO}_3\text{H}$
$\Delta m_{g,p}$	The change in water mass in the dehumidifying space (g)
Δt	Time required for the change in water mass in the dehumidifying space
λ	Water content in the dehumidifying element represented by $\text{gH}_2\text{O}/\text{gSPE}_{\text{dry}}$
ρ_s, ρ_g	Water content of the dehumidifying element of the device and water density in the air surrounding the element, respectively
$\rho_{g,p}, \rho_{g,n}$	Water content in the air facing the anode (positive electrode) and the cathode (negative electrode), respectively
$\rho_{s,p}, \rho_{s,n}$	Water contents in the anode half and cathode half of the dehumidifying element including its inner surfaces defined by a two-layer model of the element
$\rho_{g,\text{sat}}$	Saturated water density in the air
$\rho_{s,o}$	Initial water content in the dehumidifying element at switching-on of the device

Subscripts

g	Gas space
n	Negative electrode or cathode
on	At the switching-on
p	Positive electrode or anode
s	Polymer electrolytic dehumidifying element
sat	Saturated condition
st	Steady state condition
t_i	Time t_i

1 Introduction

The authors have developed an electrolytic dehumidifying device using a solid polymer electrolyte membrane (SPE membrane) as a protective measure against problems caused by high humidity. The dehumidifying device was found to effectively maintain a high reliability of electrical and electronic devices by controlling the humidity in the space containing them. The device consists of a proton-conductive solid polymer electrolyte and porous electrodes with a catalytic layer composed of noble metal particles. When a DC voltage is applied to the electrodes, the device can dehumidify the space facing the anode and humidify the space

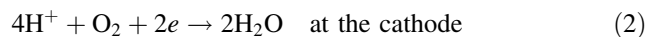
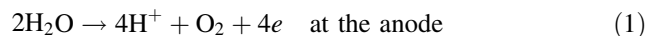
facing the cathode [1]. This type of electrolytic dehumidifying device has several advantages of no-drain, space saving and small input power compared to conventional dehumidifying techniques such as those using a Peltier element or space heater.

This paper proposes a model of the dehumidifying device using an SPE membrane. The device in the model is expressed by a two-layer membrane and electrodes on the membrane surfaces. Measurement of the membrane weight shows that the ratio of the water content in the membrane to the humidity in the surrounding air is a function of temperature under equilibrium conditions. The results for the water ratio are used to determine the parameters required for modeling. The electrical resistance of the dehumidifier is measured and is given as a function of the temperature and membrane water content. Simulation of the characteristics of the device is presented, using the model, and the results are found to agree with the measured characteristics. We also report an attempt to determine the parameters describing the dehumidifying processes.

2 Modeling of dehumidifying device

2.1 Basic equations for the model

The following reactions occur at the anode and the cathode when a DC voltage is applied to the dehumidifying device [1].



These reactions are influenced by the applied voltage, temperature and water content of the membrane. Figure 1 is a schematic diagram explaining the dehumidifying process. As shown in Fig. 1a, the device is placed on the open hole in the wall of chamber P to dehumidify the chamber. The device is operated by supplying a DC electrical source. Figure 1b shows the details of the two-layer model to represent the dehumidifying element. The dehumidifying element is represented by two parts, an anode side and a cathode side. This element can receive water from the space and also emit water to the surrounding space through its surfaces. On applying a DC electrical source to the device, water in the vicinity of the anode is decomposed and protons are produced. The protons are driven toward the cathode together with some water molecules and combined with oxygen at the cathode to produce water. As a result, the water content at the cathode side becomes higher than that at the anode and water diffuses from the cathode to the anode. Excess water at the cathode also diffuses to the space through the cathode surface. As a result, the humidity in chamber P is decreased.

The following equations are assumed for the system shown in Fig. 1.

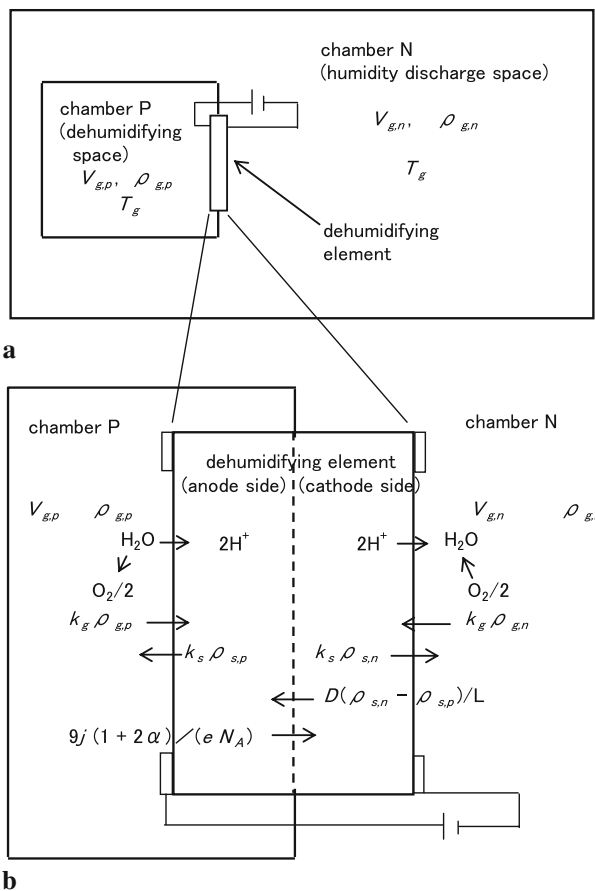


Fig. 1 System for the study of the characteristics of the dehumidifying device and a two-layer model for the device. **a** System with two spaces separated by the dehumidifying device. **b** Two-layer model for dehumidifying element made from a solid polyelectrolyte (SPE) membrane

$$\frac{d\rho_{g,p}}{dt} = \frac{S}{V_{g,p}} (k_s \rho_{s,p} - k_g \rho_{g,p}) \tag{3}$$

$$\frac{d\rho_{g,n}}{dt} = \frac{S}{V_{g,n}} (k_s \rho_{s,n} - k_g \rho_{g,n}) \tag{4}$$

$$\frac{d\rho_{s,p}}{dt} = \frac{2}{L} \left[(k_g \rho_{g,p} - k_s \rho_{s,p}) + \frac{D}{L} (\rho_{s,n} - \rho_{s,p}) - \left(\frac{1}{2} + \alpha \right) \frac{18j}{eN_A} \right] \tag{5}$$

$$\frac{d\rho_{s,n}}{dt} = \frac{2}{L} \left[(k_g \rho_{g,n} - k_s \rho_{s,n}) - \frac{D}{L} (\rho_{s,n} - \rho_{s,p}) + \left(\frac{1}{2} + \alpha \right) \frac{18j}{eN_A} \right] \tag{6}$$

$$j = \frac{I}{S} \tag{7}$$

$$I = \frac{U_s}{R_s} \tag{8}$$

$$R_s = R_s(\rho_s, T_g) \tag{9}$$

2.2 Parameter determination

Figure 2 shows a schematic diagram giving typical conditions for this system.

In the equilibrium condition at switching off of the DC voltage source, Eqs. 3–6 are then reduced as follows.

$$\rho_{g,p} = \rho_{g,n} \equiv \rho_g \tag{10}$$

$$\rho_{s,p} = \rho_{s,n} \equiv \rho_s \tag{11}$$

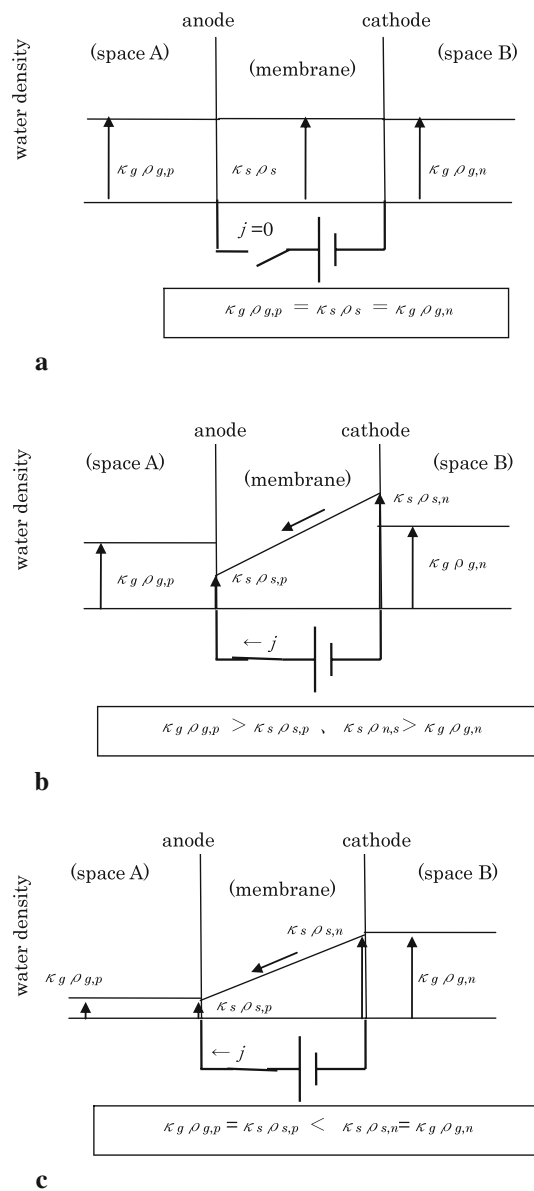


Fig. 2 Water density of dehumidifying element and its surrounding space. **a** Equilibrium condition at switch-off. **b** Dehumidifying period at switch-on. **c** Steady state condition at switch-on

$$k_s \rho_s = k_g \rho_g \quad (12)$$

The coefficient k_s in the left part of Eq. 12 is a coefficient relating to the vaporization rate of water from the element to the air and can be expressed by the following equation.

$$k_s = k_{s0} \exp(-W_s/RT_g) \quad (13)$$

W_s in Eq. 13 is the energy difference between water in the air and that in the element. Substituting (13) into (12) gives

$$\rho_s/\rho_g = k_g/k_{s0} \exp[W_s/(RT_g)] \quad (12a)$$

The values of k_g/k_{s0} and W_s can be obtained by weight measurement of the membrane at various temperatures and humidities.

After long-time operation of the device the system attains steady state as shown in Fig. 2c. Equations 3 to 6 then become

$$k_s \rho_{s,p} = k_g \rho_{g,p} \quad (14)$$

$$k_s \rho_{s,n} = k_g \rho_{g,n} \quad (15)$$

$$\frac{D}{L} (\rho_{s,n} - \rho_{s,p}) = \left(\frac{1}{2} + \alpha\right) \frac{18j}{eN_A} \quad (16)$$

Because Eqs. 14–16 are valid under steady state condition, the net transportation of water through the surfaces of the element is zero and dehumidification by the current flow is cancelled by the back diffusion of water in the dehumidifying element.

Substituting Eqs. 14 and 15 into (16), Eq. 16 gives

$$\frac{DS}{L} \frac{k_g}{k_s} (\rho_{g,n} - \rho_{g,p}) = \left(\frac{1}{2} + \alpha\right) \frac{18I_{st}}{eN_A} \quad (16a)$$

The device can dehumidify space A under the transient condition shown in Fig. 2b. The dehumidifying capability of the device is defined as the rate of water mass removed from Chamber P in Fig. 1. Thus, the capability can be obtained by the measurement of time Δt in which the humidity in the chamber changes from RH_{t_1} to RH_{t_2} . The capability can be expressed as follows.

$$\Delta m_{g,p}/\Delta t = V_{g,p} \rho_{g,sat} (RH_{t_2} - RH_{t_1})/100/\Delta t \quad (17)$$

The dehumidifying capability (17) can be transformed by making use of Eq. 3 as follows.

$$\begin{aligned} \frac{\Delta m_{g,p}}{\Delta t} &= -\frac{V_{g,p}}{(t_2 - t_1)} \int_{t_1}^{t_2} \frac{d\rho_{g,p}}{dt} dt \\ &= \frac{S}{(t_2 - t_1)} \int_{t_1}^{t_2} (k_g \rho_{g,p} - k_s \rho_{s,p}) dt \end{aligned} \quad (18a)$$

If RH_{t_1} and RH_{t_2} are selected within the range $k_g \rho_{g,p} \gg k_s \rho_{s,p}$, Eq. 18a can be approximated as follows.

$$\frac{\Delta m_{g,p}}{\Delta t} = \frac{S}{(t_2 - t_1)} k_g \int_{t_1}^{t_2} \rho_{g,p} dt = S k_g \langle \rho_{g,p} \rangle_{[t_1, t_2]} \quad (18b)$$

The k_g values can be obtained by substituting the dehumidifying capability obtained from the measurement. The value of k_{s0} can also be derived by substituting k_g into Eq. 12a.

On the other hand, the dehumidifying capability can also be expressed by making use of Eq. 5 as follows.

$$\begin{aligned} \frac{\Delta m_{g,p}}{\Delta t} &= \frac{1}{(t_2 - t_1)} \left[-\frac{LS\rho_{s,0}}{2} + \frac{9(1+2\alpha)}{eN_A} \int_{t_1}^{t_2} Idt \right. \\ &\quad \left. - \frac{DS}{L} \int_{t_1}^{t_2} (\rho_{s,n} - \rho_{s,p}) dt \right] \\ &\cong \frac{9(1+2\alpha)}{eN_A} \langle I \rangle_{[t_1, t_2]} - \frac{DS}{L} \langle \rho_{s,n} - \rho_{s,p} \rangle_{[t_1, t_2]} \end{aligned} \quad (19)$$

As seen in Eq. 19, the dehumidifying capability is the difference between dehumidification by current flow produced by the decomposition of water molecules and back diffusion occurring due to the gradient of the water content in the element. Equation 19 can be simplified to Eq. 20 when the dehumidifying capability is calculated using data measured during a period far from the steady state condition.

$$\frac{\Delta m_{g,p}}{\Delta t} \cong \frac{9(1+2\alpha)}{eN_A} \langle I \rangle_{[t_1, t_2]} - 2 \frac{DS}{L} \rho_{s,0} \quad (20)$$

Unknown factors D and α can be derived from simultaneous Eqs. 16 and 20 if we have measured the dehumidifying capability and current and can estimate the water content in the membrane by using the method shown in this section.

The dehumidifying element is composed of a proton/conductive solid polymer electrolytic membrane (Nafion 117) with porous electrodes on its surfaces. The electrodes have a catalytic layer composed of noble metal particles surrounded by Nafion to promote electrolysis.

The electrical circuit for this electrolyte with electrodes can be approximated as three parallel R-C circuits [2] as shown in Fig. 3. Elements of these parallel circuits are referred to as the resistances of the bulk, R_{bul} , grain/boundary, R_{gr} , and electrode/membrane boundary, R_{elec} , and the capacitances C_{bul} , C_{gr} and C_{elec} in parallel with these resistances. R_{bul} and R_{gr} are the resistance of the membrane itself. Usually, an impedance measurement of an electrolytic device is carried out by changing the frequency of the AC voltage.

The resistance and capacitance of the electrode/membrane boundary (R_{elec} , C_{elec}) are much larger than those of the membrane itself. Therefore, a much higher frequency

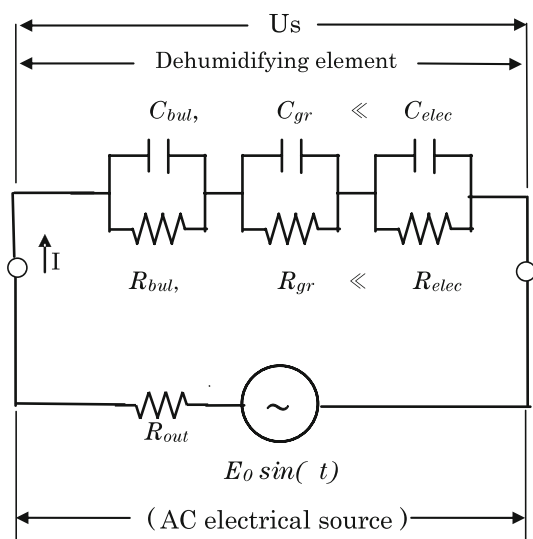


Fig. 3 Impedance measurement of dehumidifying element

of the applied AC voltage than the natural frequency of the electrode/membrane boundary circuit should be selected to evaluate the resistance of the membrane itself.

3 Experiment

3.1 Measurement of water content in SPE membrane

The measurement of the water content in the membrane (Nafion 117) was carried out using the following procedures. A membrane sheet with dimensions 12 cm × 13 cm was put in a constant humidity and constant temperature vessel for more than 2 h. The sheet was then removed from the vessel and its weight was measured. The measurements were carried out quickly because the weight gradually fell due to water vaporization. The measurements were carried out for a temperature range 283–313 K and a humidity of 40–80% in the vessel. The dry weight of the membrane was estimated by linear extrapolation of the weight measurements. The dry weight of the membrane with area 12 cm × 13 cm was estimated to be 4.92 g by linear extrapolation. The specific gravity of the dry membrane was calculated to be 1.855 g cm⁻³ assuming that the membrane thickness is constant ($L = 0.017$ cm). The water contents of the membrane were then estimated for each condition.

Figure 4 shows a typical example of time variation of the weight change of the membrane after the membrane was removed from the vessel of 303 K and 80% humidity to an environment of 303 K, 45% humidity. The time constant of the weight change of the membrane was obtained from the slope of the data. From the slope in the initial stage and around 800 s, the time constants were found to be about 600–700 s. Hence, the measurement of

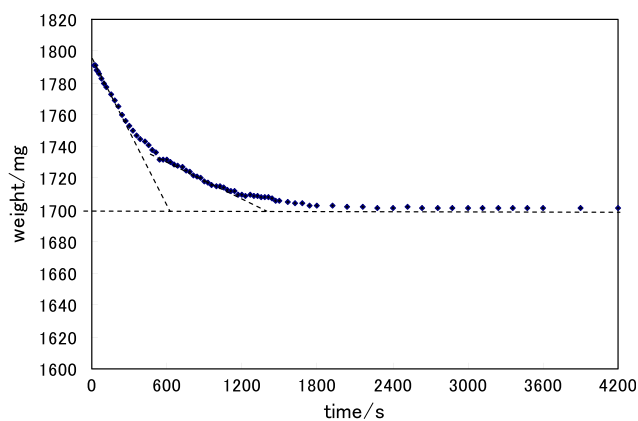


Fig. 4 Weight change of membrane (Nafion 117) after changing the condition from 303 K, 80% to 303 K, 45% at $t = 0$

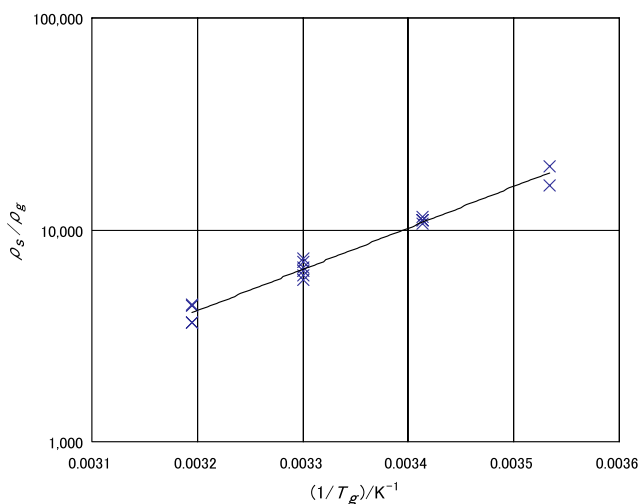


Fig. 5 Ratio of water content in SPE membrane to humidity in the surrounding air under equilibrium conditions

membrane weight in equilibrium with the environment in the temperature/humidity controlled vessel should be conducted quickly depending on the required accuracy. We adopted the value measured within 20 s after removing the membrane from the vessel as the weight in equilibrium with the environment in the vessel.

Figure 5 shows the ratio of water content in the membrane to humidity in the vessel obtained by the weight measurement. The water content ρ_s was calculated assuming that the membrane thickness was 0.017 cm. As shown in Fig. 5, the ratio ρ_s/ρ_g mainly depends on the temperature under the equilibrium condition.

The following equation can be derived from the result in Fig. 5.

$$\rho_s/\rho_g = k_g/k_{so} \exp(4500/T_g) \tag{21}$$

$$k_g/k_{so} = 2.3 \times 10^{-3} \tag{22}$$

Table 1 Dehumidifying capability of dehumidifying device (the time required for humidity change in the space of $V_{g,p}$ from RH_{t_1} to RH_{t_2})

Test case	T_g (K)	RH_{t_1} (%)	RH_{t_2} (%)	$\langle I \rangle_{[t_1,t_2]}$ (A)	Required time (s)	Dehumidifying capability (g s^{-1})	Estimated value of K_g (cm s^{-1})
Case A	303	60	50	3.86	364	4.14×10^{-4}	0.257
Case B	303	60	50	3.63	402	3.75×10^{-4}	0.233
Case C	293	80	62	3.6	600	2.59×10^{-4}	0.223
Case D	293	41	31	–	600	1.44×10^{-4}	0.244

Volume of dehumidifying space $V_{g,p} = 51 \text{ dm}^3$

Area of dehumidifying element $S = 100 \text{ cm}^2$

3.2 Determination of the coefficients k_g and k_{so} relating to water transfer across the surface of the element

To determine the coefficients k_g and k_{so} , an experiment to determine the dehumidifying capability of the device was carried out using the experimental set-up shown in Fig. 1. A dehumidifying element with area 100 cm^2 and a chamber of volume 51 dm^3 were used. The time required for the reduction of the humidity in the chamber from RH_{t_1} to RH_{t_2} was measured and the dehumidifying capability was then calculated. The value of k_g was then estimated using Eq. 18b.

Table 1 shows the results for the dehumidifying capability of the device. Coefficient k_g related to the diffusion velocity of water from the air to the membrane can be estimated by substituting the dehumidifying capability into Eq. 18b. These results are also shown in Table 1. Estimated values of k_g are around 0.24 cm s^{-1} for 293–303 K and do not depend so much on temperature and humidity in the measured ranges. Substituting $k_g = 0.24 \text{ cm s}^{-1}$ into Eq. 22, the coefficient k_{so} was obtained as follows.

$$k_g = 0.24 \text{ (cm s}^{-1}\text{)} \quad (23)$$

$$k_{so} = 1.1 \times 10^2 \text{ (cm s}^{-1}\text{)} \quad (24)$$

3.3 Determinations of the diffusion coefficient of water in the membrane and the number of water molecules carried by a proton moving to the cathode

The system in Fig. 1 reaches a steady state condition described by Eqs. 14–16 within several hours of operation.

Table 2 Physical quantities under steady state conditions (humidifying space $V_{g,n}$ was kept at humidity RH_{t_1} during the experiment)

Test case	T_g (K)	RH_{t_1} (%)	RH_{st} (%)	I_{t_0} (A)	I_{st} (A)	$D/(1+2\alpha)$ ($\text{cm}^2 \text{ s}^{-1}$) (calculated by Eq. 16a)
Case C	293	80	3.3	10	1.6	1.79×10^{-7}
Case D	293	41	<0.5	8	0.8	1.70×10^{-7}
Case E	303	65	0.5	10	1.5	1.91×10^{-7}
Case F	303	61	0.8	9.5	1.2	1.64×10^{-7}

T_g ambient temperature, RH_{t_1} initial humidity in the spaces $V_{g,p}$ and $V_{g,n}$, RH_{st} humidity in the space $V_{g,p}$ under steady state condition, I_{st} current under the steady state condition

Physical quantities under the steady state condition were measured using the experimental setup shown in Fig. 1. Table 2 shows the physical quantities measured under steady state conditions.

By substituting measured quantities shown in Table 2 into Eq. 16a, the values of $D/(1+2\alpha)$ for each case were estimated and are also shown in Table 2. The estimated values are about $1.8 \times 10^{-7} \text{ cm}^2 \text{ s}^{-1}$ for 293–303 K. The values do not depend much on temperature and humidity in the range.

$$D/(1+2\alpha) = 1.8 \times 10^{-7} \text{ (cm}^2 \text{ s}^{-1}\text{)} \quad (25)$$

The values of α and D were separately obtained by substituting Eq. 25 into Eq. 20 as follows:

$$\alpha = 1.3 \quad (26)$$

$$D = 6.2 \times 10^{-7} \text{ (cm}^2 \text{ s}^{-1}\text{)} \quad (27)$$

The obtained values for α and D are assumed to be valid at least within the range 293–303 K.

3.4 Determination of electrical resistance of the dehumidifying element

The resistance of the dehumidifying element with area 100 cm^2 was measured under different temperatures and humidities. An HP 4192A LF impedance analyzer (YHP) was used. The impedance was measured using the AC internal voltage of the analyzer. The AC voltage was supplied to the element via 50Ω of internal resistance of the analyzer. Figure 6 shows the impedances measured by varying the frequency of the AC voltage. The resistance of

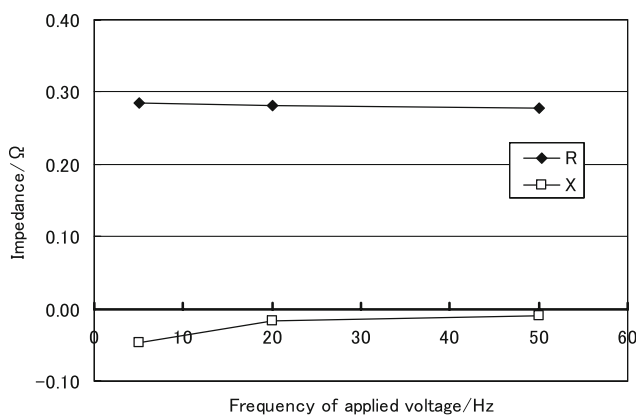


Fig. 6 Impedance measurement of dehumidifying element with area 100 cm²

the element was found to be about 0.28 Ω. An AC voltage of 1 V was selected for the measurement. Therefore, the actual voltage applied to the element itself was about 0.28/50 V. Electrolysis of water cannot occur under the conditions for resistance measurement, because the voltage is much less than the electrolysis voltage (1.23 V).

The resistance values measured are around 0.28 Ω and do not depend much on the voltage frequency from 5 to 50 Hz. The measured reactance values are from −0.01 to −0.05 Ω. The reactance is much smaller than the resistance in the frequency range. As a result the element can be expressed as a series Rs-Cs circuit composed of a

resistance of around 0.28 Ω and a capacitance of around 0.3–0.7 F. The capacitance estimated to be 0.3–0.7 F should be the electrode/membrane boundary capacitance C_{elec} , and the resistance of around 0.28 Ω should be the resistance of the membrane (R_m), that is, the sum of R_{bul} and R_{gr} . Thus, the resistance of the membrane itself can be obtained by applying an AC voltage.

An AC voltage at a frequency of 5 Hz was selected to measure the resistance of the element to avoid the effect of the parallel capacitance of the element itself. The measurements were conducted in the temperature range 303–333 K and the humidity range 50–90%. The measured resistances are shown in Table 3 and Fig. 7. The best fit equations for the element of area 100 cm² are also expressed in Fig. 7 and are unified in the following form.

$$R_m = \frac{0.67 \times 10^{-3} \exp(670/T_g)}{\rho_s} + 0.173 \text{ (}\Omega\text{)} \tag{28}$$

Here, ρ_s is in g cm^{−3}.

It can be seen that the resistance changes linearly with the inverse of the water content in the element and also depends on ambient temperature.

In the case where the DC voltage applied to the element is high enough to produce electrolysis, the whole resistance of the element is the sum of the resistance of the membrane expressed by Eq. 28 and the electrode/membrane boundary resistance, R_{elec} . The resistance R_{elec} is assumed to also be affected by the water content in the boundary, especially

Table 3 Measured electrical resistance of the dehumidifying element of area 100 cm²

T_g (K)	Ambient humidity (%)	ρ_g (g cm ^{−3})	ρ_s (g cm ^{−3})	λ (H ₂ O/SO ₃ H)	δ (gH ₂ O/gSPE)	Resistance (Ω (meas.))
303	50	1.48×10^{-5}	0.095	3.2	0.052	0.237
303	60	1.78×10^{-5}	0.114	3.8	0.062	0.225
303	70	2.08×10^{-5}	0.133	4.5	0.073	0.217
303	80	2.38×10^{-5}	0.152	5.1	0.083	0.212
303	90	2.67×10^{-5}	0.171	5.8	0.093	0.208
313	50	2.49×10^{-5}	0.099	3.3	0.054	0.228
313	60	2.99×10^{-5}	0.119	4.0	0.065	0.218
313	70	3.48×10^{-5}	0.139	4.7	0.076	0.212
313	80	3.98×10^{-5}	0.158	5.3	0.087	0.208
313	90	4.48×10^{-5}	0.178	6.0	0.097	0.204
323	50	4.04×10^{-5}	0.103	3.5	0.056	0.224
323	60	4.84×10^{-5}	0.124	4.2	0.068	0.215
323	70	5.65×10^{-5}	0.144	4.9	0.079	0.209
323	80	6.46×10^{-5}	0.165	5.6	0.090	0.205
323	90	7.27×10^{-5}	0.185	6.3	0.101	0.201
333	50	6.36×10^{-5}	0.107	3.6	0.058	0.219
333	60	7.64×10^{-5}	0.128	4.3	0.070	0.211
333	70	8.91×10^{-5}	0.150	5.0	0.082	0.206
333	80	1.02×10^{-4}	0.171	5.8	0.093	0.202
333	90	1.15×10^{-4}	0.192	6.5	0.105	0.199

Ps: calculated by Eq. 21

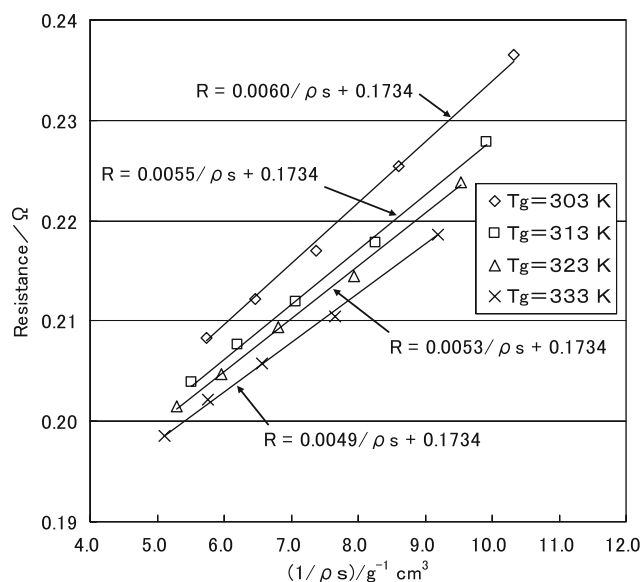


Fig. 7 Electrical resistance of dehumidifying element with area 100 cm² vs. water content in the membrane

the water content in the vicinity of the anode because the water content near the anode directly affects the amount of electrolysis. Therefore, the resistance R_{elec} can be assumed to be proportional to the inverse of the water content at the anode. The entire resistance of the element can then be expressed as follows.

$$R_s = R_{elec} + R_m = \frac{A(T_g)}{\rho_{s,p}} + Eq. 28 \quad (29)$$

Though we do not have additional data on $A(T_g)$, the same expression as Eq. 28 was applied to $A(T_g)$ to simulate the characteristics of the dehumidifying device.

4 Simulation of the characteristics of the dehumidifying device

Experiments to determine the characteristics of the dehumidifying device were carried out using the experimental setup in Fig. 1. A chamber of volume 51 dm³ shown in Fig. 1 was located in a temperature/humidity controlled vessel. The time dependence of the humidity and temperatures for both the inner volume and the outer volume of the vessel and the current were then measured. The experimental results were compared to the simulation based on the idea shown in Sect. 2.

Figure 8 shows a comparison of the experimental and calculated results for the change in humidity and current after switching on of the dehumidifying device when the ambient temperature and humidity were 293 K and 80%, respectively. The dehumidification of the chamber started at $t = 0$, and the current was rapidly reduced in the early

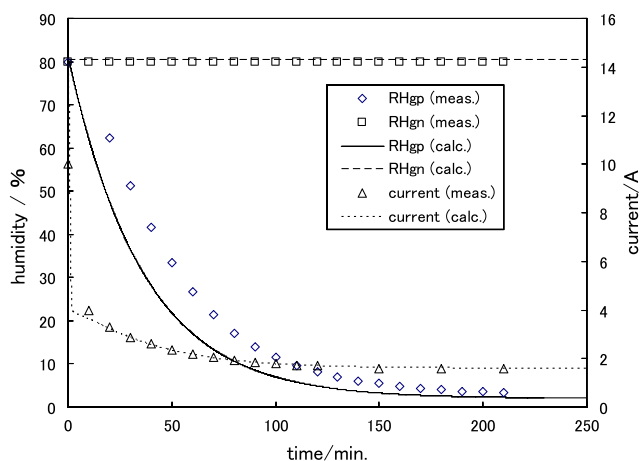


Fig. 8 Comparison of experiment and simulation on the humidity change of 51 dm³ space under the outer condition of 293 K, 80% humidity

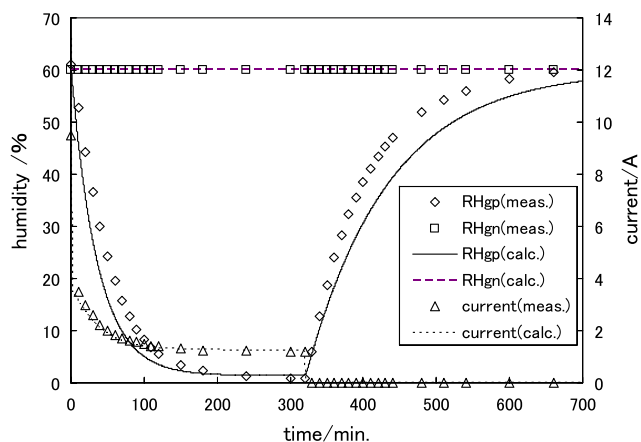


Fig. 9 Comparison of experiment and simulation on the humidity change of 51 dm³ space under the outer condition 303 K, 60% humidity

stages. Thereafter, the current and humidity of the chamber were reduced more slowly to the steady state. The changes in the humidity and the current in the calculation are similar to the measured ones. Figure 9 shows another example of the changes in the humidity and current after switch on at $t = 0$ and switch off at around 320 min. After switch off, the humidity in the chamber recovered to the ambient humidity. The time variations in the humidity of the dehumidifying chamber and the current for simulation are similar to those of the experiment. Figure 10 shows detailed comparison of the initial change in current and water content between the experiment and calculation under the condition of 293 K, 40%. The initial change by calculation agrees well with that by experiment.

From the simulation, the rapid reduction of current in the early stages just after switching on of the device is found to be caused by the reduction of water content in the element

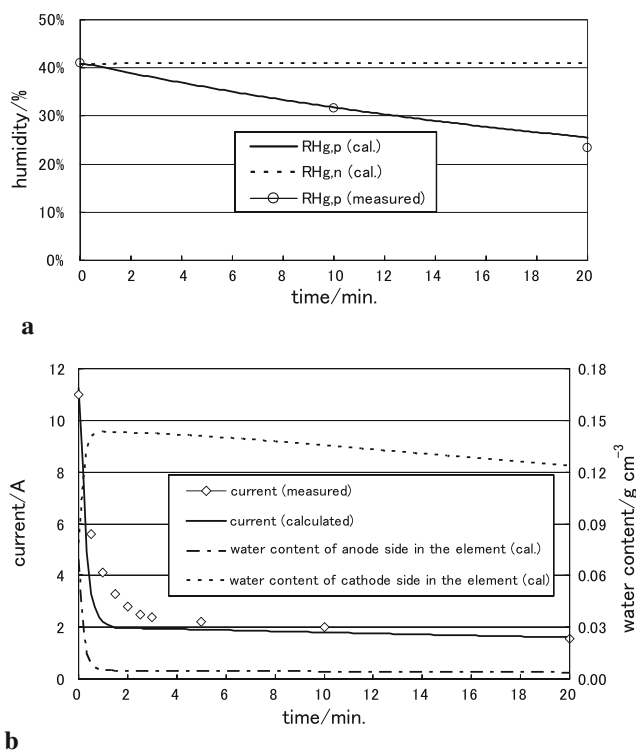


Fig. 10 Initial change in current and water contents of the dehumidifying element with area 100 cm² during dehumidification of a chamber with volume 51 dm³. **a** Humidity change in the chamber. **b** Changes in current and water content

near the anode that causes the increase in resistance of the element. This is caused by electrolysis of water in the element. As a result, the water content becomes lower at the anode side and higher at the cathode side. Thus a gradient of water content is formed in the element. The rapid reduction of current occurs during this period. After forming the gradient in the water distribution, dehumidification of the space begins and a current change begins to follow the humidity change in the space.

Figure 11 shows a comparison of the steady state current calculated by the model with the measurement. The steady state current flowing in the dehumidifying element of area 100 cm² was measured under the condition in which the dehumidifying element was exposed in open air (that means $\rho_{g,p} = \rho_{g,n}$). The calculated results are similar to those of the measurement. Thus, this model seems to be valid at least in the range shown in Fig. 11.

5 Discussion

The two-layer model expresses both the transient characteristics and the steady state characteristics of the dehumidification of the device using an SPE membrane

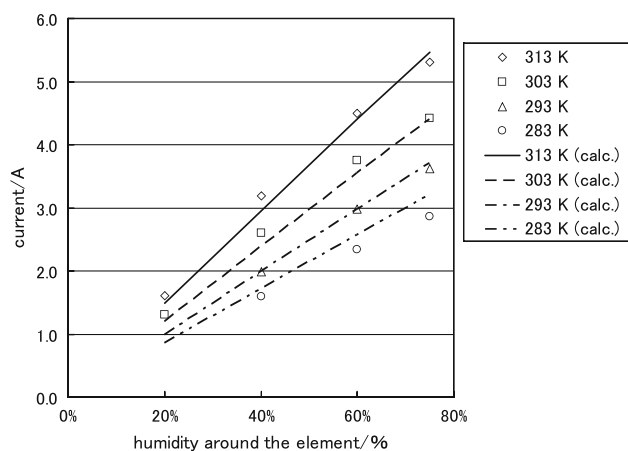


Fig. 11 Steady state current flowing in the dehumidifying element exposed in open air ($S = 100 \text{ cm}^2$, under the condition $\rho_{g,p} = \rho_{g,n}$)

very well. Thus the model can be assumed to reflect the real characteristics of the SPE dehumidifying device.

The ratio of the water content in the membrane to that in the ambient air mainly depends on the temperature under the equilibrium condition. The difference in potential energy W_s ($= 4500 R$) of water between that in the air and that in the membrane (Nafion 117) is estimated to be 37.3 kJ mol⁻¹ from the curve in Fig. 5. This is slightly lower than the vaporization energy of liquid water ($= 40.7 \text{ kJ mol}^{-1}$). The energy W_s is around the vaporization energy of liquid water; therefore, the water content in the membrane also depends on the relative humidity. Hinatsu et al. [3] reported previously that the water content of Nafion 117 depends on the relative humidity of the space surrounding the membrane. Water contents in our experiment are compared with those by Hinatsu et al. in Table 4. The water content in the present work agrees with the results of Hinatsu et al.

The water vapor transmission rate (q) is defined as the amount of water vapor (Q) passing through a membrane per unit time and unit area and is given by Eq. 30. From the two-layer model, the water vapor permeability coefficient (P) of the dehumidifying element is given by Eq. 31 as a function of parameters used in the model.

Table 4 Comparison of water content vs. relative humidity

RH (%)	Our experiment		Results of Hinatsu et al. [3]	
	gH ₂ O/gSPE	molH ₂ O/molSO ₃ H	gH ₂ O/gSPE	molH ₂ O/molSO ₃ H
40	0.04	2.4	0.05	3
60	0.06–0.07	3.8–4.3	0.06	4
80	0.08–0.09	5.1–5.9	0.09	6

Table 5 Typical values by simulation

	Steady state condition shown in (2c) of Fig. 2	Transient condition shown in (2b) of Fig. 2
T_g (K)	303 K	303 K
$RH_{g,p}$ (%)	0.5	55
$RH_{g,n}$ (%)	60	60
I (A)	1.3	3.7
Water by current	$1.2 \times 10^{-4} \text{ g s}^{-1}$	$3.5 \times 10^{-4} \text{ g s}^{-1}$
Water by electro-osmotic drag	$3.1 \times 10^{-4} \text{ g s}^{-1}$	$9.0 \times 10^{-4} \text{ g s}^{-1}$
Water by back diffusion	$4.3 \times 10^{-4} \text{ g s}^{-1}$	$8.4 \times 10^{-4} \text{ g s}^{-1}$
Net water transported	0 g s^{-1}	$4.1 \times 10^{-4} \text{ g s}^{-1}$

$$q \equiv \frac{Q}{St} = \frac{D}{L} \frac{k_g}{k_s + 2D/L} (\rho_{g,n} - \rho_{g,p}) \quad (30)$$

$$= \frac{D}{L} \frac{k_g m_o}{k_s + 2D/L} \frac{(p_{g,n} - p_{g,p})}{RT_g} = P \frac{(p_{g,n} - p_{g,p})}{L}$$

$$P \equiv D \frac{k_g}{k_s + 2D/L} \frac{m_o}{RT_g} \quad (31)$$

The diffusion coefficient obtained by the present study is $6.2 \times 10^{-7} \text{ cm}^2 \text{ s}^{-1}$ for Nafion 117 with the water molecules per sulfonate ($\lambda = 2\text{--}6$ ($\text{H}_2\text{O}/\text{SO}_3\text{H}$)) under temperatures of 293–303 K. Yeo et al. [4] measured the diffusion coefficient of water in Nafion 115 with $\lambda = 22$ and gave the following equation.

$$D = 6.0 \times 10^{-3} \times \exp(-20.2 \times 10^3 / (RT_g)) \quad (\text{cm}^2 \text{ s}^{-1}) \quad (32)$$

This equation gives $1.9 \times 10^{-6} \text{ cm}^2 \text{ s}^{-1}$ at $T_g = 303 \text{ K}$. Zawodzinski et al. [5] also show water diffusion coefficients in Nafion 117 as a function of λ and give coefficients of 0.6×10^{-6} to $3.7 \times 10^{-6} \text{ cm}^2 \text{ s}^{-1}$ for λ from 2 to 6 at 303 K. Nguyen et al. [6] investigated the diffusion coefficients of water in Nafion of different thicknesses under different temperatures. Nguyen et al. [6] showed that the diffusion coefficient for Nafion 117 with a water content of 2–6% of dry membrane weight is 1.5×10^{-7} – $6.0 \times 10^{-7} \text{ cm}^2 \text{ s}^{-1}$ at 333 K. According to these reports, the diffusion coefficient depends on temperature and water content. The authors did not show a temperature dependence of the diffusion coefficient because they did not have sufficient data for the determination of this dependence. However, the author's opinion is that the diffusion coefficient in the membrane depend on temperature as reported by those papers. Our simulation by the two-layer model can be improved by introducing a dependence on temperature and water content.

The number of water molecules α carried by a proton moving toward the cathode is referred to as the electroosmotic drag coefficient [5]. We obtained 1.3 from the experiment under temperatures of 293–303 K and relative humidities of 40–80%. Zawodzinski et al. [5] reported that

the electro-osmotic drag coefficient for Nafion 117 exposed to liquid water at 303 K is 2.5–2.9 with $\lambda = 22$ and they suggest a substantial decrease in the electroosmotic drag coefficient as the water content is lowered. The difference in our result from theirs may result from the difference in the water contents in our element from that of Zawodzinski et al.

Typical values of our results under steady state and transient conditions in the environment of 303 K, 60% are shown in Table 5. Under the steady state condition, water transported by both current and electroosmotic drag is cancelled by back diffusion. As a result, the dehumidifying capability at the steady state condition is zero. The dehumidifying capability under the transient condition shown in Table 5 is calculated to be $4.1 \times 10^{-4} \text{ g s}^{-1}$. From our estimation by simulation, the amount of water transported by electroosmotic drag is nearly cancelled by that from back diffusion.

The electrolytic membrane of the element is covered by porous electrodes on both of its surfaces. Therefore, the actual area to transport water across the surfaces may be less than the area S of the membrane itself. We assume in this paper that the water transportation area across the surfaces is S for simplification. The D and α estimated by the present paper may be influenced by this assumption.

The electrical resistance of the dehumidifying element was measured using an impedance analyzer with a frequency controllable AC source. Anantaraman et al. [7] reported the effect of humidity on the conductivity of Nafion 117. They measured the conductance by a high frequency impedance method. Electrical resistivity at 303 K measured by Anantaraman et al. depends much more on the relative humidity in the surrounding air than that obtained in the present paper. However, the values are nearly the same around a relative humidity of 50%.

6 Conclusions

A two-layer model for a dehumidifying device making use of a solid polymer electrolyte (SPE) membrane is presented. By comparing the model simulation with experimental

measurements, the model is found to express the characteristics of the device well. This model is effective in understanding the behavior of such a device using an SPE membrane. The ratio of the water content in the SPE membrane to that in ambient air under equilibrium conditions is presented as a function of temperature. The electrical resistance of the dehumidifying element using the SPE membrane was measured by making use of an AC voltage at 5 Hz. The resistance was expressed as a function of temperature and the water content in the membrane. The resistance is used for estimation of the current flowing through the dehumidifying element and provides resistance values similar to those of the device when in operation. The authors cannot reflect on the temperature dependency of the diffusion of water and the electroosmotic drag in the

membrane. The simulation could be improved by introducing this dependency.

References

1. Yamauchi S, Nakatani H, Sakuma S, Mitsuda K (2000) *Trans IEE Jpn* 120-A(5):607
2. Ikuta H (2000) *Electrochemistry* 68(5):356
3. Hinatsu JT, Mizuhara M, Takenaka H (1994) *J Electrochem Soc* 141(6):1493
4. Yeo SC, Eisenberg A (1977) *J Appl Polym Sci* 21:875
5. Zawodzinski TA, Derouin C, Radzinski S, Sherman RJ, Smith VT, Springer TE, Gottesfeld S (1993) *J Electrochem Soc* 140(4):1041
6. Nguyen T, Guante J, Vanderborgh N (1989) *Mater Res Soc Symp Proc* 135:367
7. Anantaraman AV, Gardner CL (1996) *J Electroanal Chem* 414:115